

# Activity and Activity Coefficient of Iron Oxides in the Liquid FeO-Fe<sub>2</sub>O<sub>3</sub>-CaO-SiO<sub>2</sub> Slag Systems at Intermediate Oxygen Partial Pressures

HECTOR M. HENAO and KIMIO ITAGAKI

At present, there is a scarcity of data on the activities of iron oxides in the FeO-Fe<sub>2</sub>O<sub>3</sub>-CaO-SiO<sub>2</sub> slag system at intermediate oxygen partial pressures and temperatures relevant to sulfide smelting and nonferrous metallurgy. The present study provides relevant data at temperatures between 1573 and 1673 K and partial pressures of oxygen between 10<sup>-9</sup> and 10<sup>-4</sup> atm. The experiments were carried out by equilibrating the slag in a CO-CO<sub>2</sub> gas mixture in a platinum crucible, after which the phases of all the experimental samples, including the platinum foil, were analyzed by electron probe microanalysis (EPMA). Where only liquid phase or liquid phase and tridymite (SiO<sub>2</sub>) were observed, wet chemical analysis was used to determine the ratio of (mass pct Fe<sup>2+</sup>)/(mass pct Fe<sup>3+</sup>). Activity and activity coefficients for FeO (liquid) and FeO<sub>1.33</sub> (solid) were calculated. Tendencies of the effect of the (CaO/SiO<sub>2</sub>) ratio, temperature, and oxygen partial pressure on these thermochemical quantities are discussed in this article.

DOI: 10.1007/s11663-007-9077-7

© The Minerals, Metals & Materials Society and ASM International 2007

## I. INTRODUCTION

THERMODYNAMIC information of activity and activity coefficient are important to the development of new metallurgical processes. Furthermore, this information can assist in improving the computer simulation models. Most of the experimental data for the activity of iron oxides in the FeO-Fe<sub>2</sub>O<sub>3</sub>-CaO-SiO<sub>2</sub> system reported in the literature<sup>[1,2]</sup> cover the areas of temperatures and oxygen partial pressures relevant to iron production. However, there exist few reported data on thermodynamic information at the intermediate oxygen partial pressures and temperatures in nonferrous metal production.

Experimental phase diagrams of the FeO-Fe<sub>2</sub>O<sub>3</sub>-CaO-SiO<sub>2</sub> slag at intermediate oxygen partial pressures have already been reported by the authors.<sup>[3]</sup> However, this work was insufficient for the calculation of quantitative relationships between the phase equilibrium diagrams and the thermodynamic properties of that system. The present study builds on the previous work and provides relevant data of activity and activity coefficient of iron oxides in the FeO-Fe<sub>2</sub>O<sub>3</sub>-CaO-SiO<sub>2</sub> system at temperatures between 1573 and 1673 K and partial pressures of oxygen between 10<sup>-9</sup> and 10<sup>-4</sup> atm.

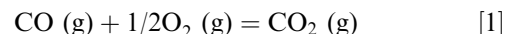
The experimental method consisted of equilibration of the slag in a platinum crucible, quenching, and analysis of the phases by electron probe microanalysis (EPMA). This is a proven method for determining phase

diagrams for iron slag systems.<sup>[4]</sup> However, in combination with the analysis of composition of platinum foil by EPMA and that of (mass pct Fe<sup>3+</sup>/mass pct Fe<sup>2+</sup>) ratio by wet chemical analysis, the method should prove equally reliable in obtaining data on activity and activity coefficient of iron oxides in iron oxide liquid solution.

This proposed method of determination of activities and activity coefficients has the additional advantage that every experiment measurement is complete in itself, as opposed to a measurement obtained by the integration of the Gibbs-Duhem equation reported for a number of FeO-Fe<sub>2</sub>O<sub>3</sub>-CaO-SiO<sub>2</sub> related systems.<sup>[1,5-7]</sup>

## II. EXPERIMENTAL METHOD AND PROCEDURE OF CALCULATION

Details of the experimental method and procedure were reported in the previous article.<sup>[3]</sup> A schematic diagram of the furnace is shown in Figure 1. A premelted FeO-Fe<sub>2</sub>O<sub>3</sub>-CaO-SiO<sub>2</sub> mother slag was mixed with Fe<sub>2</sub>O<sub>3</sub>, CaO, and SiO<sub>2</sub> to obtain the required initial composition and was held in a platinum foil crucible with 20-mm height, 6-mm diameter, and 0.03-mm thickness. The sample was heated at the desired temperature and oxygen pressure. The temperature was controlled within 2 K by a SCR controller with a Pt/Pt-Rh thermocouple. CO<sub>2</sub>-CO gas mixtures were used to control the partial pressure of oxygen according to Reaction [1].<sup>[8]</sup>



$$\Delta G^\circ / J = -279,710 + 84.08 T$$

The gas mixture, which was regulated using a capillary flow meter, was introduced into the reaction

HECTOR M. HENAO, Research Fellow, is with the Pyrosearch Centre, School of Engineering, The University of Queensland, Brisbane, QLD 4072, Australia. Contact e-mail: h.henaozapata@uq.edu.au KIMIO ITAGAKI, Professor Emeritus, is with the Institute of Multidisciplinary Research for Advanced Materials, Tohoku University, Sendai 980-8577, Japan.

Manuscript submitted March 7, 2006.  
Article published online August 31, 2007.

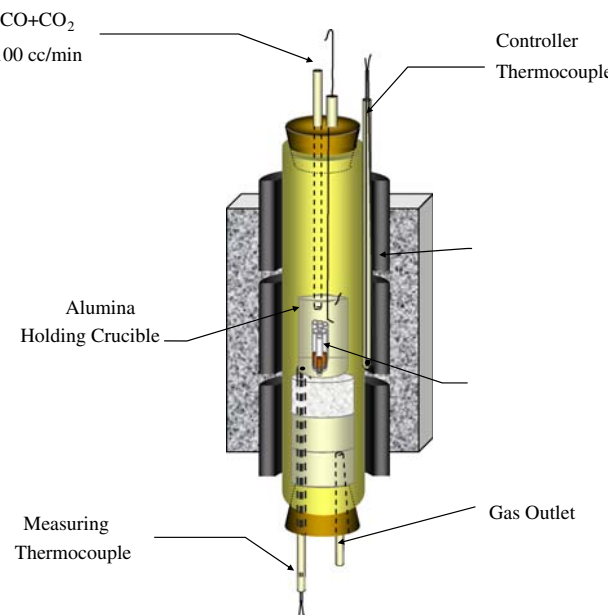


Fig. 1—Experimental apparatus.

chamber through an alumina tube with a flow rate of  $1.7 \times 10^{-6} \text{ m}^3/\text{s}$ . Previous experiments indicated that the equilibrium with the platinum crucible could be obtained in 86.4 ks, as is indicated in the profile of Fe obtained at different holding times shown in Figure 2. Thus, after the holding time of 86.4 ks, the sample was taken out from the upper side of the furnace and quenched in a jet stream of argon.

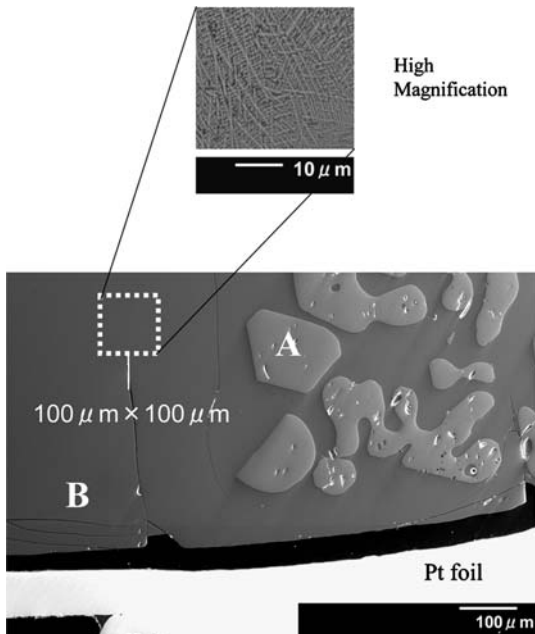


Fig. 2—Analysis of glassy slag composition (A: wüstite, and B: glassy slag).

The sample was subsequently divided vertically in two parts. One vertical section of the quenched sample was mounted on epoxy resin, polished, and analyzed by optical microscope. The quantitative chemical composition of mass pct CaO, mass pct SiO<sub>2</sub>, and mass pct Fe of the different phases present was analyzed by EPMA at a minimum of eight places on each sample. The observed crystals and the platinum foil were analyzed by the conventional EPMA technique of point analysis. The liquid phase, which as indicated in Figure 3 is segregated during quenching, was analyzed with the method of scanner area analysis. The EPMA analysis was undertaken using a JEOL\* 8200L with wavelength

\*JEOL is a trademark of Japan Electron Optics Ltd., Tokyo.

dispersive detectors. An acceleration voltage of 15 kV and a prove current of 15 nA were used. The standards were wollastonite ( $\text{CaSiO}_3$ ) for Ca and Si, hematite ( $\text{Fe}_2\text{O}_3$ ) for Fe in slag and metallic iron, and platinum for the analysis of the platinum crucible.

Where the optical microscope analysis indicated that only liquid slag phase or liquid and tridymite ( $\text{SiO}_2$ ) were present, the remaining section of the sample was separated from the crucible and prepared for the wet chemical analysis to obtain the mass pct  $\text{Fe}^{3+}$ /mass pct  $\text{Fe}^{2+}$  ratio. In this analytical method, the finely ground samples were dissolved in hydrochloric hydrofluoric acid in an environment of argon. Two aliquots of the dissolved sample were prepared using the 1, 10-phenanthroline method—one for the total mass pct Fe and the other for mass pct  $\text{Fe}^{2+}$ . The  $\text{Fe}^{3+}/\text{Fe}^{2+}$  mass pct ratio was determined by spectrophotometry (Spectrophotometer Hitachi model 100-40, Japan) at a wavelength of 508 nm.

#### A. Methodology of Calculation

The calculation of activities for the slag system is based on the chemical Reaction [2],

$$\text{FeO}_X \text{ (in slag)} = \text{Fe (in Pt)} + x/2\text{O}_2 \quad [2]$$

which controls the content of iron in the platinum crucible in equilibrium with slag. Data on the activity of  $\text{FeO}$  (l, s) or  $\text{FeO}_{1.33}$  (s) in the binary Fe-O system and the equilibrium constant for Reaction [2] are reported in the literature.<sup>[9-11]</sup> However, to use this equation, the iron oxides in equilibrium with liquid slag must be considered pure components. This is proven to be the case, with good approximation, later on. This information was used to determine a polynomial relationship between the content of iron in the platinum crucible, measured at different temperatures, and oxygen partial pressures, on the one hand, and the corresponding activity coefficient of iron, as reported in the literature, on the other.

The activity of iron oxide in the liquid in these experiment in which only the liquid phase or liquid and tridymite ( $\text{SiO}_2$ ) phases are present was derived from the following chemical Reactions [3] and [4]:

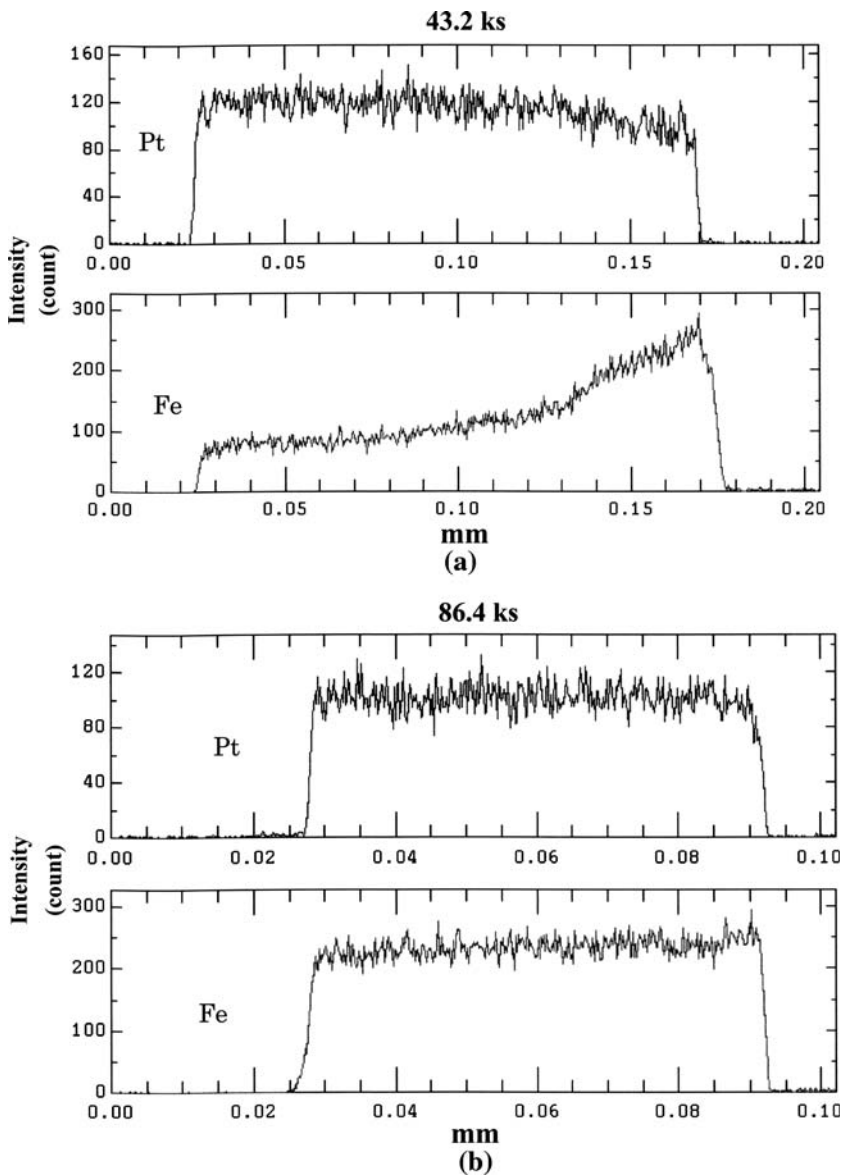
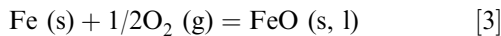


Fig. 3—Profiles of platinum and iron concentrations in a cross section of platinum foil at 1573 K and  $p\text{O}_2$  of  $10^{-8}$  at different holding times. (The left and right sides present the outside and inside of the platinum crucible, respectively.).



In this equation, the activity coefficient of iron was calculated by using the established polynomial relationship and the content of iron in the platinum crucible found in the afore-mentioned experiments.

The activity coefficient of iron oxide in liquid slag was calculated using the obtained activities together with the mole fraction composition of  $\text{FeO}-\text{Fe}_2\text{O}_3-\text{CaO}-\text{SiO}_2$ . The mole fraction was calculated by a combination of the composition obtained by EPMA and the  $\text{Fe}^{3+}/\text{Fe}^{2+}$  ratio.

### III. RESULTS AND DISCUSSION

Two characteristic features of the  $\text{FeO}-\text{Fe}_2\text{O}_3-\text{SiO}_2-\text{CaO}$  system are (1) a number of different crystalline phases are present and (2) the range of solubility of  $\text{SiO}_2$  and  $\text{CaO}$  in wustite and magnetite is relatively limited.<sup>[12,13]</sup> According to the phase rule at a given temperature and oxygen partial pressure, three condensed phases coexist at an invariant point (coexistence of three condensed phases) and two phases coexist along a univariant line (coexistence of two condensed phases). In this study, thermodynamic information for the univariant lines and invariant points for some of these crystalline phases in equilibrium with the liquid slag was obtained. The results can be separated according to the following equilibrium relations:

- (a) equilibrium among platinum crucible, liquid slag, and magnetite ( $\text{FeO}_{1.33}$ ) or wüstite ( $\text{FeO}$ );
- (b) equilibrium between platinum crucible and liquid  $\text{FeO}-\text{Fe}_2\text{O}_3-\text{SiO}_2-\text{CaO}$  slag; and
- (c) equilibrium among platinum crucible, liquid  $\text{FeO}-\text{Fe}_2\text{O}_3-\text{SiO}_2-\text{CaO}$  slag, and tridymite ( $\text{SiO}_2$ ) or dicalcium silicate ( $2\text{CaO} \cdot \text{SiO}_2$ ).

Detailed experimental conditions are indicated in Table I, and the experimental results of this equilibrium relation will be described in detail in the following section A.

#### A. Equilibrium among Platinum Crucible, Liquid Slag, and Magnetite ( $\text{FeO}_{1.33}$ ) or Wüstite ( $\text{FeO}$ )

This equilibrium experiment provides the necessary data to establish a relationship between the activity coefficient of iron in the  $\text{FeO}-\text{Fe}_2\text{O}_3-\text{SiO}_2-\text{CaO}$  system and the content of iron in the platinum crucible. The validity of the obtained equation was corroborated by taking the results of the calculation of the standard free energy of the formation of magnetite ( $\text{FeO}_{1.33}$ ) and those of the calculation of the activity of wustite ( $\text{FeO}$ ) obtained by using the relationship expression and

comparing these with the corresponding data reported in the literature. In addition, the solubility of  $\text{CaO}$  and  $\text{SiO}_2$  in magnetite ( $\text{FeO}_{1.33}$ ) and wüstite ( $\text{FeO}$ ) in equilibrium with liquid slag was measured.

The experimental results of these equilibria are shown in Tables II, III, IV, V, VI, VII, VIII and represented in Figures 4, 5, 6, 7, 8, 9, 10, 11. At intermediate oxygen partial pressures, the liquid phase contains both ferrous and ferric oxides. Measurements of chemical analysis of phases by EPMA provide information only on the total cation content, as reported in the tables of results. Thus, the total iron oxide ( $\text{FeO} + \text{Fe}_2\text{O}_3$ ) indicated in Figures 4 and 7 through 10 was calculated as 100 wt pct- $\text{CaO}$  wt pct- $\text{SiO}_2$  wt pct. In Tables II and III, the samples with an asterisk indicate the invariant points for the equilibrium among liquid  $\text{FeO}-\text{Fe}_2\text{O}_3-\text{SiO}_2-\text{CaO}$  slag, magnetite ( $\text{FeO}_{1.33}$ ), and silica.

The calculated Gibbs energies of formation of magnetite ( $\text{FeO}_{1.33}$ ),  $\Delta G^\circ \text{FeO}_{1.33}$  (solid), are shown in Tables II, III, IV, VII, and VIII, while the calculated activities of  $\text{FeO}$  (liquid) in the  $\text{FeO}-\text{Fe}_2\text{O}_3-\text{SiO}_2-\text{CaO}$  slag liquid solution are given in Tables V and VI. The procedure to calculate  $\Delta G^\circ \text{FeO}_{1.33}$  and the activity for  $\text{FeO}$  are explained in the following section 1.

**Table I.** Liquid Slag Equilibrium Phase Assemblage with Solid Phases in This Study

Equilibrium	Temperature (°C)	Oxygen Partial Pressure (atm)	Obtained Information
Platinum crucible, liquid slag, and magnetite	1573	$10^{-4}, 10^{-6}$ , and $10^{-7}$	tie-line between liquid slag and magnetite, and $\Delta G^\circ \text{FeO}_{1.33}$
	1573 and 1673	$10^{-6}$	tie-line between liquid slag and magnetite, and $\Delta G^\circ \text{FeO}_{1.33}$
Platinum crucible, liquid slag, and wüstite	1573	$10^{-8}$ and $10^{-9}$	tie-line between liquid slag and wüstite, and $\Delta G^\circ \text{FeO}_{1.33}$ and $a_{\text{FeO}}$
Platinum crucible and liquid slag	1673	$10^{-8}$	$a_{\text{FeO}}$ and $\gamma_{\text{FeO}}$
	1673	$10^{-6}$	$a_{\text{FeO}}, a_{\text{FeO}1.33}$ , and $\gamma_{\text{FeO}}$
	1673	$10^{-8}$	$a_{\text{FeO}}$ and $\gamma_{\text{FeO}}$
Platinum crucible, liquid slag, and silica	1573	$10^{-6}$	$a_{\text{FeO}}, a_{\text{FeO}1.33}$ , and $\gamma_{\text{FeO}}$
	1573	$10^{-8}$	$a_{\text{FeO}}$ and $\gamma_{\text{FeO}}$
Platinum crucible, liquid slag, and $2\text{CaO} \cdot \text{Fe}_2\text{O}_3$	1573	$10^{-7}$ and $10^{-8}$	$a_{\text{FeO}}$ and $\gamma_{\text{FeO}}$

**Table II.** Equilibrium among Platinum Crucible, Liquid  $\text{FeO}-\text{Fe}_2\text{O}_3$ -Slag, and Magnetite at 1573 K and  $p\text{O}_2$  of  $3.43 \times 10^{-4}$  atm

Number	Crucible Fe	(Mass Pct)					
		Magnetite Crystal		Slag			$\Delta G^\circ \text{FeO}_{1.33}$ (kJ/mol)
		SiO <sub>2</sub>	CaO	Fe	SiO <sub>2</sub>	CaO	
A-7*	3.0	0.31	0.0	36.72	37.5	10.4	-204.0
A-8	2.6	0.21	0.0	35.17	36.7	15.3	-210.3
A-9	2.5	0.22	0.0	33.26	36.6	17.3	-211.5
A-10	2.9	0.23	0.0	32.49	38.7	17.9	-205.0
A-11	2.6	0.26	0.0	33.52	37.1	17.6	-208.1

\*Invariant point: equilibrium among platinum crucible, liquid slag, magnetite, and silica.

**Table III. Equilibrium among Platinum Crucible, Liquid FeO-Fe<sub>2</sub>O<sub>3</sub>-CaO-SiO<sub>2</sub> Slag, and Magnetite at 573 K and  $p_{O_2}$  of 10<sup>-6</sup> atm**

Number	Crucible Fe	(Mass Pct)						$\Delta G^\circ FeO_{1.33}$ (kJ/mol)	
		Magnetite Crystal			Slag				
		SiO <sub>2</sub>	CaO	Fe	SiO <sub>2</sub>	CaO			
C-1	6.8	0.47	0.0	44.08	35.5	4.0		-206.2	
C-2	7.00	0.49	0.0	42.20	35.5	4.8		-204.8	
C-3*	6.6	0.40	0.0	41.13	35.9	5.1		-207.0	
C-4*	6.6	0.38	0.0	40.51	36.4	6.0		-207.2	
C-5	7.0	0.46	0.0	44.34	35.7	4.9		-204.5	
C-6	6.9	0.36	0.0	41.14	35.7	9.1		-205.4	
C-7	6.9	0.40	0.0	41.41	35.8	8.6		-205.1	
C-8	6.8	0.30	0.0	39.94	35.7	8.8		-205.8	
C-9	7.1	0.14	0.06	29.47	37.6	22.5		-204.0	
C-10	6.7	0.15	0.10	26.53	38.1	24.5		-206.4	
C-11	6.6	0.11	0.10	24.77	38.4	26.3		-207.2	
C-12	6.8	0.26	0.0	34.01	37.4	16.6		-205.9	
C-13	7.1	0.22	0.0	35.62	37.5	15.2		-204.2	
C-14	6.8	0.05	0.16	24.57	35.1	32.7		-206.3	
C-15	—	0.10	0.19	23.95	35.4	33.1		—	
C-16	6.9	0.01	2.49	58.02	0.0	18.3		-205.4	
C-17	7.0	0.03	2.5	59.47	0.0	18.4		-204.7	
C-18	6.8	0.01	2.5	57.27	0.0	18.4		-205.9	
C-19	7.2	0.03	2.2	58.99	1.94	18.9		-203.7	
C-20	6.7	0.03	2.4	57.24	0.28	18.5		-206.5	
C-21	6.7	0.08	0.15	24.06	34.2	32.2		-206.8	
C-22	6.6	0.25	0	36.48	36.5	10.7		-207.5	
C-23	—	0.18	0.02	—	—	—		—	
C-24	6.5	0.10	0.13	26.78	33.7	32.2		-208.0	
C-25	—	0.12	0.18	26.23	32.4	32.5		—	
C-26*	6.5	0.39	0	44.39	35.9	6.2		-207.7	
C-27	—	0.15	0	37.26	34.7	17.0		—	

\*Invariant point: equilibrium among platinum crucible, liquid slag, magnetite, and silica.

**Table IV. Equilibrium among Platinum Crucible, Liquid FeO-Fe<sub>2</sub>O<sub>3</sub>-CaO-SiO<sub>2</sub> Slag, and Magnetite at 1573 K and  $p_{O_2}$  of 10<sup>-7</sup> atm**

Number	Crucible Fe	Mass Pct						$\Delta G^\circ FeO_{1.33}$ (kJ/mol)	
		Magnetite Crystal			Slag				
		SiO <sub>2</sub>	CaO	Fe	SiO <sub>2</sub>	CaO			
D-1	10.6	0.18	0	45.3	27.1	12.2		-205.6	
D-2	10.6	0.03	0.17	35.6	23.1	26.7		-205.8	
D-3	10.7	0.07	0.08	36.1	25.7	26.1		-205.2	
D-4	—	0.15	0	40.5	29.6	16.4		—	
D-5	—	0.27	0	—	—	—		—	
D-6	10.9	0.16	0	37.9	29.2	22.0		-204.3	
D-7	10.8	6	0	41.5	29.6	16.3		-204.9	
D-8	10.8	—	—	57.1	23.9	0.0		-204.8	
D-9	10.8	—	—	47.6	27.8	—		-204.8	
D-10	10.7	—	—	43.8	29.5	—		-205.4	

The compositions of solid wüstite and magnetite phases in equilibrium with the liquid slag are shown in Tables II through VIII. The solubility of SiO<sub>2</sub> in wüstite and magnetite was found to be less than 0.5 mass pct. The solubility of CaO was also low, except in the FeO-Fe<sub>2</sub>O<sub>3</sub>-CaO subsystem, where the solubility can increase to as

much as 2 mass pct. Thus, magnetite and wüstite can be considered to be pure components in the following thermodynamic calculations. A graphical example of those results at 1573 K and 10<sup>-6</sup> and 10<sup>-8</sup> atm are indicated in Figure 4. The black dots represent the composition of the liquid slag, while the open circles

**Table V. Equilibrium among Platinum Crucible, Liquid FeO-Fe<sub>2</sub>O<sub>3</sub>-CaO-SiO<sub>2</sub> Slag, and Wüstite at 1573 K and  $p_{O_2}$  of 10<sup>-8</sup> atm**

Number	Crucible Fe	Mass Pct					
		Wüstite Crystal			Slag		
		SiO <sub>2</sub>	CaO	Fe	SiO <sub>2</sub>	CaO	$a_{FeO}$
E-1	15.1	0.04	0.55	53.6	11.3	17.2	0.64
E-2	15.4	0.05	0.37	50.8	13.9	18.3	0.71
E-3	—	0.18	0.06	43.0	25.8	19.9	—
E-4	15.2	0.18	0.03	44.1	24.2	19.3	0.66
E-5	15.0	0.21	0.02	43.7	25.0	18.5	0.62
E-6	14.9	0.19	0.03	39.4	29.0	19.9	0.61
E-7	15.4	0.17	0	41.5	26.9	18.5	0.70
E-10	15.4	0.50	0	50.8	23.0	9.6	0.71
E-11	15.3	0.37	0.01	48.8	25.4	10.9	0.68
E-12	15.5	0.20	0.13	38.3	25.3	17.0	0.72
E-14	15.3	0.61	0.00	62.0	19.2	0	0.67
E-15	14.8	0.10	0.35	44.73	20.0	21.3	0.60
E-16	14.7	0.21	0.13	40.05	26.9	20.5	0.60

**Table VI. Equilibrium among Platinum Crucible, Liquid FeO-Fe<sub>2</sub>O<sub>3</sub>-CaO-SiO<sub>2</sub> Slag, and Wüstite at 1573 K and  $p_{O_2}$  of 10<sup>-9</sup> atm**

Number	Crucible Fe	Mass Pct					
		Wüstite Crystal			Slag		
		SiO <sub>2</sub>	CaO	Fe	SiO <sub>2</sub>	CaO	$a_{FeO}$
F-1	21.6	0.38	0.00	66.7	8.8	0	0.87
F-2	21.1	0.40	0.05	63.7	—	—	0.77
F-3	21.6	0.45	0.11	60.9	5.1	0.14	0.87
F-4	21.3	0.52	0.22	55.6	5.4	0	0.83
F-5	21.1	0.49	0.32	51.0	3.1	0.88	0.79
F-6	21.5	0.55	0.52	43.6	2.4	4.23	0.86
F-7	21.5	0.00	0.29	69.5	1.6	60.1	0.85

**Table VII. Equilibrium among Platinum Crucible, Liquid FeO-Fe<sub>2</sub>O<sub>3</sub>-CaO-SiO<sub>2</sub> Slag, and Magnetite at 1623 K and  $p_{O_2}$  of 10<sup>-6</sup> atm**

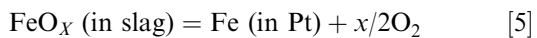
Number	Crucible Fe	Mass Pct					
		Magnetite Crystal			Slag		
		SiO <sub>2</sub>	CaO	Fe	SiO <sub>2</sub>	CaO	$\Delta G^{\circ}FeO_{1.33}$ (kJ/mol)
G-1	8.6	0.18	0	56.4	26.3	0	-201.9
G-2	8.7	0.11	0	45.1	30.2	8.8	-201.2
G-3	8.5	0	0.31	35.3	21.3	29.9	-202.4
G-4	9.0	0	0.60	55.9	3.1	15.6	-199.9
G-5	8.9	0.1	0.01	41.5	29.9	14.1	-200.2
G-6	8.9	0.02	0.16	36.9	28.0	23.3	-200.2
G-7	9.2	0.02	0.31	31.6	26.7	29.4	-199.7
G-8	8.8	—	0.70	58.7	0.27	16.3	-200.5

represent that of the crystals. Notice that for a schematic illustration of the tie-lines, the CaO and SiO<sub>2</sub> composition were plotted on two different scales—one for the liquid slag and the other for the iron oxide.

### 1. Activity coefficient of iron in Pt-Fe alloy

At equilibrium, the content of platinum in the slag is negligible. However, the platinum crucible forms the

solid solution of Pt-Fe when in contact with the slag according to Reaction [5]:



This reaction indicates that the content of iron in platinum crucible depends entirely on the temperature, oxygen partial pressure, and slag composition.

**Table VIII. Equilibrium among Platinum Crucible, Liquid FeO-Fe<sub>2</sub>O<sub>3</sub>-CaO-SiO<sub>2</sub> Slag, and Magnetite at 1623 K and  $p_{O_2}$  of  $10^{-6}$  atm**

Number	Crucible Fe	Mass Pct						$\Delta G^{\circ} \text{FeO}_{1.33}$ (kJ/mol)	
		Magnetite Crystal		Slag					
		SiO <sub>2</sub>	CaO	Fe	SiO <sub>2</sub>	CaO			
H-1	10.5	0.02	0.19	67.0	0.16	11.1	-198.0		
H-2	10.5	0.31	0.08	62.1	2.3	0	-198.1		
H-3	10.6	0.23	0.26	57.9	0	4.0	-197.5		
H-4	10.6	0.04	0.16	65.6	0.80	9.6	-197.7		
H-5	10.4	0.28	0.00	65.1	4.8	0.0	-197.6		
H-6	10.7	0.32	0.16	59.6	2.8	0.40	-197.2		
H-7	10.6	0.27	0.23	58.9	4.4	0	-197.7		
H-8	10.6	0.23	0.23	59.1	2.8	1.2	-197.2		
H-9	10.8	0.01	0.20	67.3	0.23	11.2	-196.5		

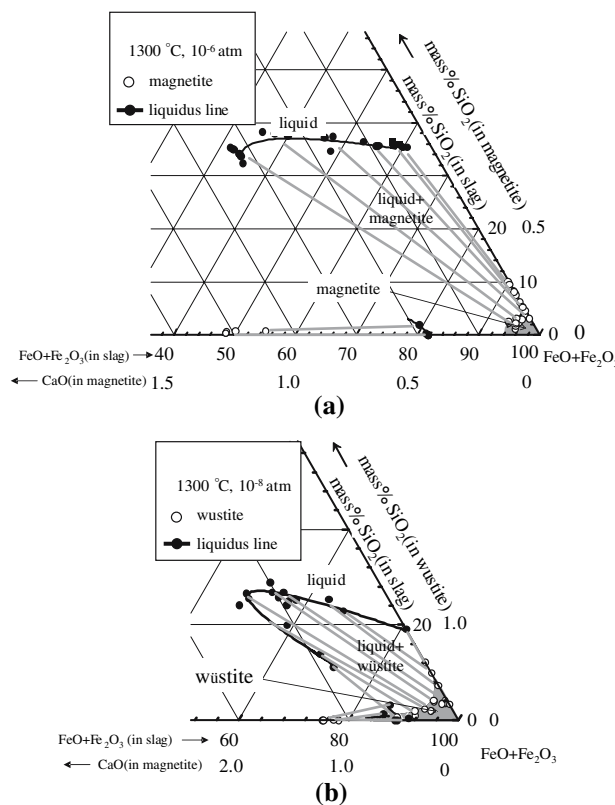


Fig. 4—Tie-lines for equilibrium between wüstite and liquid slag at 1573 K and at  $p_{O_2}$  of  $10^{-8}$  and  $10^{-6}$  atm.

The activity of iron in the Pt-Fe alloy in equilibrium with the slag should therefore be identical to that in the precipitated iron oxide phase of wüstite or magnetite, provided that the same reference state is used in both phases. The activity coefficient of iron can be calculated according to Eq. [6]

$$\gamma_{\text{Fe}}(\text{s}) = a_{\text{Fe}} / N_{\text{Fe}} \text{ (in Pt)} \quad [6]$$

where  $\gamma_{\text{Fe}}(\text{s})$  indicates the activity coefficient of gamma-iron in the Pt-Fe solid solution,  $a_{\text{Fe}}$  corresponds

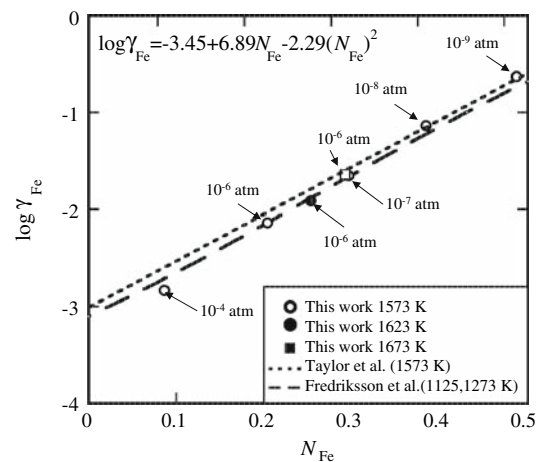


Fig. 5—Activity coefficient of Fe in the Pt-Fe crucible.

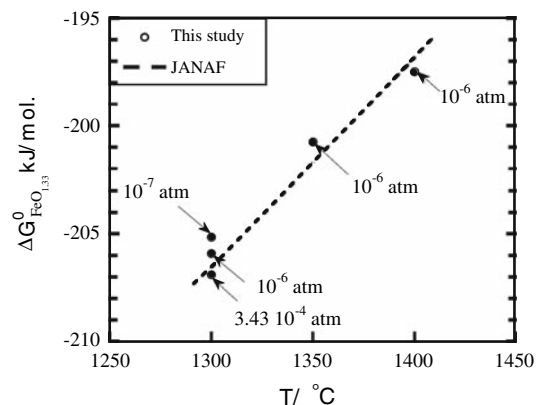


Fig. 6—Gibbs free energy of formation of solid crystal  $\text{FeO}_{1.33}$ .

to the activity of iron in the Fe-O system (or Pt-Fe alloy), and  $N_{\text{Fe}}$  (in Pt) to the mole fraction of iron in the platinum crucible equilibrated with the liquid slag and the crystal of magnetite or wüstite.

The crystals of wüstite and magnetite can be treated as the pure components, as previously shown. The  $a_{\text{Fe}}$

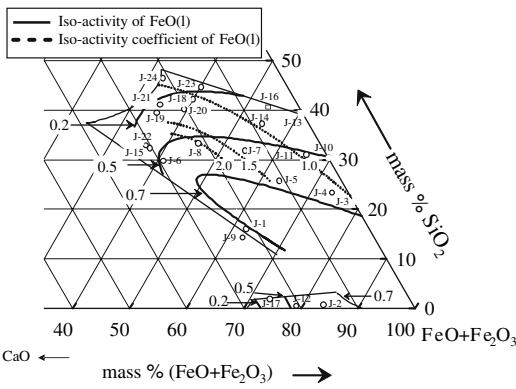


Fig. 7—Activity and activity coefficient of FeO at 1573 K and  $p_{O_2}$  of  $10^{-8}$  atm.

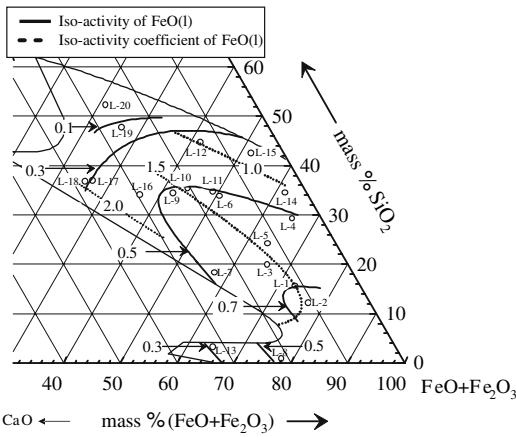


Fig. 8—Activity and activity coefficient of FeO at 1673 K and  $p_{O_2}$  of  $10^{-8}$  atm.

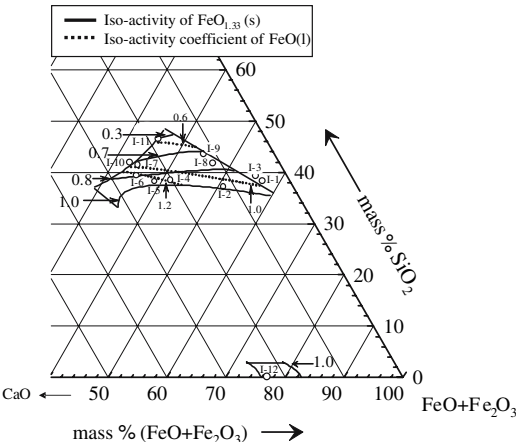


Fig. 9—Activity of FeO and activity coefficient of  $FeO_{1.33}$  at 1573 K and  $p_{O_2}$  of  $10^{-6}$  atm.

data selected by Spencer and Kubaschewski<sup>[10]</sup> were used in Eq. [3]. The results of the calculated activity of iron are shown in Figure 5. The relationship between  $\gamma_{Fe}$  (s) and  $NFe$  can be expressed by Eq. [7]:

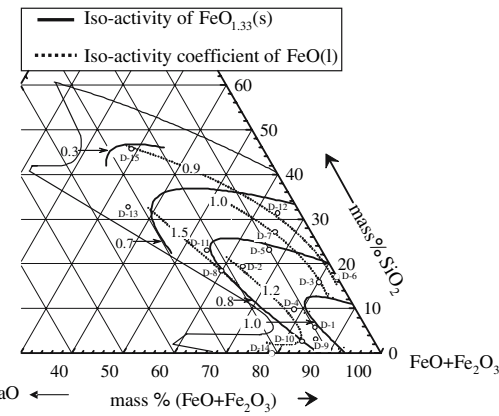


Fig. 10—Activity of FeO and activities coefficient of  $FeO_{1.33}$  at 1673 K and  $p_{O_2}$   $10^{-6}$  atm.

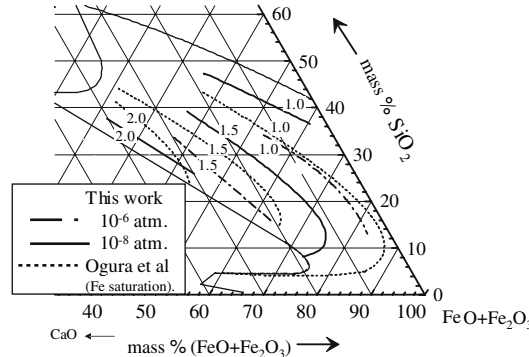


Fig. 11—Isoactivity coefficient lines for FeO at 1673 K and  $p_{O_2}$  of  $10^{-6}$  and  $10^{-8}$  atm and at iron saturation.

$$\log \gamma_{Fe} = -3.45 + 6.89NFe \text{ (in Pt)} - 2.29(NFe \text{ (in Pt)})^2 \\ 0.08 < NFe \text{ (in Pt)} < 0.5 \quad [7]$$

A number of authors have reported on the relationship between the content of iron in the platinum-iron alloy and the activity coefficient of iron.<sup>[14,15]</sup> Considering the significant discrepancies in their findings and in order to validate the equation obtained in the present study, the standard free energy of formation of  $FeO_{1.33}$  (s) was calculated using the preceding formula [4]. The chemical reaction is expressed by Eq. [8]



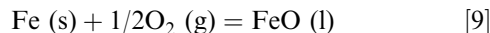
$$K_8 = aFeO_{1.33}(s)/(aFePO_2^{2/3})$$

$$\Delta G^\circ = -RT \ln(1/\gamma_{Fe} \text{ (s)} NFe \text{ (in Pt)} p_{O_2}^{2/3}) \\ \text{with } aFeO_{1.33} \text{ (s)} = 1$$

where  $aFeO_{1.33}$  (s) represents the activity of solid  $FeO_{1.33}$  and  $\Delta G^\circ$  the free energy of formation of magnetite.

The results of  $\Delta G^\circ \text{FeO}_{1.33}$  (s) calculated by Eq. [6] are shown in Tables II, III, IV, VII, and VIII. Figure 6 shows the average value obtained at every set of oxygen partial pressure and temperature. Within a standard deviation of 2 kJ/mol, the present results are in good agreement with those reported in the JANAF database,<sup>[16]</sup> as indicated in Figure 6.

Equation [5] was further validated by a calculation of the activity of FeO (l) and by comparing the results with those reported in the literature. The activity of FeO (l) at 1573 K and the oxygen partial pressures of  $10^{-8}$  and  $10^{-9}$  atm were calculated using Eq. [9]:



$$K_9 = a\text{FeO (l)} / (\gamma\text{Fe (s)} N\text{Fe (in Pt)} p\text{O}_2^{1/2})$$

where  $a\text{FeO (l)}$  indicates the activity of FeO (l) with the standard state of FeO (l) as the pure Fe-O melt in equilibrium with gamma-Fe, and  $p\text{O}_2$  indicates the controlled oxygen partial pressure. The values of  $K_9$  reported by Schuhmann<sup>[17]</sup> were used.

Darken<sup>[9]</sup> reports the values of  $a\text{FeO(l)}$  with 0.70 and 0.83 at 1573 K and the oxygen partial pressures of  $10^{-8}$  and  $10^{-9}$  atm, respectively. This shows good agreement with the average values of 0.66 and 0.83, as listed in Tables VI and VI, respectively.

### B. Equilibrium between Platinum Crucible and Liquid Slag

This equilibrium provides data on the activities and activity coefficients of FeO (l) and  $\text{FeO}_{1.33}$  (s) in the liquid FeO- $\text{Fe}_2\text{O}_3$ -CaO-SiO<sub>2</sub> slag. These data were obtained from the measurement of iron content in the platinum crucible combined with the mole fraction of the FeO- $\text{Fe}_2\text{O}_3$ -CaO-SiO<sub>2</sub> system.

The FeO- $\text{Fe}_2\text{O}_3$ -CaO-SiO<sub>2</sub> slag system at intermediate oxygen partial pressures contains both ferrous and ferric oxides. Measurements of phases by EPMA provide information only on the total cation content. Consequently, a wet chemical analysis was carried out

to determine the  $\text{Fe}^{2+}/\text{Fe}^{3+}$  mass pct ratio. The results are shown in Tables IX to XII.

The ratios ranged between 0.2 and 1.7, indicating that all the experimental points fall within the FeO- $\text{Fe}_2\text{O}_3$ -CaO-SiO<sub>2</sub> quaternary system. These ratios were combined with the composition of the slag provided by the EPMA analysis to determine the composition of FeO- $\text{Fe}_2\text{O}_3$ -CaO-SiO<sub>2</sub> slag. Tables IX through XII include those data and also include  $a\text{FeO (l)}$ ,  $a\text{FeO}_{1.33}$  (s), and the activity coefficient of FeO (l) calculated by Eqs. [4] through [6] and the values of  $K$  indicated in Table XIII.

Every point in Tables IX through XII is represented with its respective code in the (FeO- $\text{Fe}_2\text{O}_3$ )-CaO-SiO<sub>2</sub> pseudo-ternary system shown in Figures 7 through 10. It can be noticed that, between the experimental accuracy of this experimental work, there is no difference by calculating the (FeO +  $\text{Fe}_2\text{O}_3$ ) from 100 wt pct-CaO wt pct-SiO<sub>2</sub> wt pct or by calculating the total iron oxide by combining the total content of iron obtained by the EPMA and the ratio of  $\text{Fe}^{3+}/\text{Fe}^{2+}$  obtained by wet chemical analysis. Figures 7 through 10 also include the estimated isoactivity and isoactivity coefficient lines. The liquidus lines for the equilibrium with the iron oxides were taken as a base reference.

Thus, isoactivity lines of FeO were drawn at an oxygen partial pressure of  $10^{-8}$  atm and temperatures of 1573 and 1673 K, and isoactivity lines of  $\text{FeO}_{1.33}$  (s) were drawn at  $10^{-6}$  atm and temperatures of 1573 and 1673 K. The liquidus lines in Figures 8 and 10 correspond to those reported in the *Slag Atlas*<sup>[18]</sup> at 1673 K and at iron saturation. The liquidus line at 1573 K and the oxygen partial pressures of  $10^{-6}$  and  $10^{-8}$  atm (Figures 7 and 9) correspond to those estimated in the previous work.<sup>[3]</sup>

It was found that, at a given temperature and at oxygen partial pressure, the values of the isoactivity coefficient lines increase with increasing content of CaO in the slag. In a given composition at the oxygen partial pressure  $10^{-6}$  or  $10^{-8}$  atm, there is no appreciable change in the isoactivity lines when the temperature increases from 1573 to 1673 K. However, it was apparent that an increase in the oxygen partial pressure from  $10^{-8}$  to  $10^{-6}$  atm displaces the isoactivity lines toward the CaO

Table IX. Equilibrium between Platinum Crucible and Liquid FeO- $\text{Fe}_2\text{O}_3$  CaO-SiO<sub>2</sub> Slag at 1573 K and  $p\text{O}_2$  of  $10^{-6}$  atm

Number	Mass Pct Fe in Pt	Slag Composition, Mass Pct				Slag Composition Mol Fraction				Activity and Activity Coefficient		
		Fe	SiO <sub>2</sub>	CaO	Fe <sup>3+</sup> /Fe <sup>2+</sup>	N SiO <sub>2</sub>	N CaO	N FeO	N FeO <sub>1.5</sub>	$a\text{FeO}_{1.33}$	$a\text{FeO}$	$\gamma\text{FeO}$
I-1	6.9	42.0	38.5	4.72	0.44	0.43	0.06	0.36	0.16	1.07	0.35	0.99
I-2	6.7	35.6	37.4	13.9	0.41	0.41	0.16	0.30	0.13	0.99	0.33	1.07
I-3	6.7	43.1	39.5	5.33	0.35	0.44	0.06	0.37	0.13	0.99	0.32	0.88
I-4	6.6	32.6	38.7	20.3	0.48	0.41	0.23	0.24	0.12	0.95	0.31	1.30
I-5	6.3	29.1	38.4	23.03	0.58	0.41	0.26	0.21	0.12	0.82	0.27	1.29
I-6	6.1	27.4	6.00	25.50	0.45	0.42	0.29	0.20	0.09	0.73	0.24	1.17
I-8	5.5	33.6	43.8	12.05	0.49	0.44	0.27	0.19	0.10	0.54	0.18	0.92
I-9	5.6	26.3	41.6	3	0.36	0.46	0.13	0.30	0.11	0.56	0.18	0.60
I-7	5.4	34.6	42.0	11.3	0.44	0.47	0.14	0.27	0.12	0.51	0.17	0.63
I-10	5.3	23.1	43.1	25.4	0.44	0.45	0.28	0.18	0.08	0.50	0.16	0.88
I-11	4.5	28.1	46.7	18.3	0.40	0.49	0.21	0.21	0.09	0.30	0.10	0.46
I-12	—	40.1	40.4	10.7	—	0.44	0.12	0.32	0.11	—	—	—

**Table X. Equilibrium between Platinum Crucible and Liquid FeO-Fe<sub>2</sub>O<sub>3</sub>-CaO-SiO<sub>2</sub> Slag at 1573 K and pO<sub>2</sub> of 10<sup>-8</sup> atm**

Number	Mass Pct Fe in Crucible	Slag Composition, Mass Pct				Slag Composition, Mol Fraction				Activity and Activity Coefficient	
		Fe	SiO <sub>2</sub>	CaO	Fe <sup>3+</sup> /Fe <sup>2+</sup>	NSiO <sub>2</sub>	N <sub>CaO</sub>	N <sub>FeO</sub>	N <sub>FeO<sub>1.5</sub></sub>	$a_{FeO}$	$\gamma_{FeO}$
J-1	15.1	44.77	16.16	21.56	0.66	0.18	0.26	0.34	0.22	0.65	1.92
J-2	15.0	63.39	0.84	15.72	0.00	—	—	—	—	0.64	—
J-3	15.0	59.92	21.65	0.00	0.32	0.25	0.00	0.57	0.18	0.64	1.12
J-4	15.0	55.26	23.42	2.93	0.39	0.27	0.04	0.50	0.19	0.62	1.25
J-5	14.9	48.49	24.79	11.03	0.34	0.29	0.13	0.43	0.15	0.61	1.42
J-6	14.7	29.83	30.89	29.75	0.42	0.32	0.33	0.25	0.10	0.58	2.35
J-7	14.6	40.4	31.95	13.88	0.22	0.35	0.16	0.40	0.09	0.56	1.41
J-8	14.6	33.49	33.44	21.34	0.41	0.36	0.25	0.28	0.11	0.56	2.00
J-9	14.5	45.76	14.40	23.09	0.00	—	—	—	—	0.55	—
J-10	14.2	53.41	30.40	0.00	0.17	0.35	0.00	0.56	0.09	0.51	0.91
J-11	14.2	49.63	31.14	3.55	0.14	0.35	0.04	0.53	0.07	0.50	0.95
J-12	14.2	58.24	0.64	20.58	0.14	0.01	0.26	0.34	0.39	0.50	1.47
J-13*	13.6	48.07	39.44	0.40	0.15	0.44	0.00	0.48	0.07	0.43	0.89
J-14*	13.5	40.49	37.34	8.19	0.15	0.41	0.10	0.43	0.07	0.41	0.97
J-15	13.3	27.04	32.41	30.33	0.00	—	—	—	—	0.39	—
J-16*	13.3	39.77	40.65	5.49	0.13	0.45	0.06	0.43	0.06	0.39	0.89
J-17	12.9	52.38	2.02	24.55	2.50	0.02	0.31	0.19	0.48	0.35	1.83
J-18	12.9	29.51	42.27	17.84	0.19	0.45	0.20	0.29	0.06	0.35	1.18
J-19	12.9	23.47	37.82	32.78	0.42	0.39	0.36	0.17	0.07	0.35	1.99
J-20	12.7	28.75	40.32	20.42	0.24	0.43	0.23	0.27	0.07	0.32	1.18
J-21	12.7	25.6	41.19	24.19	0.21	0.43	0.27	0.25	0.05	0.32	1.31
J-22	12.6	27.04	32.99	30.77	0.00	—	—	—	—	0.31	—
J-23	11.7	30.84	44.74	15.19	0.19	0.48	0.17	0.29	0.06	0.23	0.80
J-24	11.0	25.01	46.52	21.00	0.22	0.49	0.24	0.23	0.05	0.18	0.80

\*Equilibrium among the platinum crucible, liquid slag, and silica saturation.

corner. Ogura *et al.*<sup>[2]</sup> reported activity coefficients of FeO in equilibrium with solid iron in the FeO-CaO-SiO<sub>2</sub> system (iron saturation) at 1673 K determined by measuring the chemical potential of FeO by the emf method. In Figure 11, the results of Ogura *et al.*<sup>[2]</sup> and the results of the present experiment at the same temperature and at 10<sup>-6</sup> and 10<sup>-8</sup> atm are compared. The isoactivity lines show a similar general tendency.

#### C. Equilibrium among Platinum Crucible, Liquid Slag, and Silica or Dicalcium Ferrite

Activities of FeO (l) in liquid FeO-Fe<sub>2</sub>O<sub>3</sub>-CaO-SiO<sub>2</sub> slag in this equilibrium were calculated with Eqs. [4] and [5]. The results are shown in Table XIV. The results of equilibrium among platinum crucible, liquid slag, and silica at 1573 K and the oxygen partial pressures of 10<sup>-8</sup> and 10<sup>-7</sup> atm are shown in Table X (marked with an asterisk) and Table XIV. The reported results of Michael and Schuhmann<sup>[18]</sup> in the FeO-Fe<sub>2</sub>O<sub>3</sub>-SiO<sub>2</sub> system under the condition of silica saturation were 0.37 and 0.33 at 1573 K and oxygen partial pressures of 10<sup>-8</sup> and 10<sup>-7</sup> atm. The present study obtained the results of 0.43 and 0.31, respectively.

For the FeO-Fe<sub>2</sub>O<sub>3</sub>-CaO system under the condition of calcium ferrite (2CaO · Fe<sub>2</sub>O<sub>3</sub>) saturation at 1573 K and between 10<sup>-8</sup> and 10<sup>-6</sup> atm, Takeda *et al.*<sup>[7]</sup> report a value of activity for FeO (l) between 0.2 and 0.3. The result obtained in this study is between 0.2 and 0.32.

The data obtained in the present study are in reasonable agreement with the data reported in the literature.

#### IV. CONCLUSIONS

The activity and activity coefficient of iron oxides in the liquid FeO-Fe<sub>2</sub>O<sub>3</sub>-CaO-SiO<sub>2</sub> slag system were measured at temperatures of 1573 to 1673 K and oxygen partial pressures of 10<sup>-4</sup> to 10<sup>-9</sup> atm. The experiments were carried out by equilibrating the slag in a CO-CO<sub>2</sub> gas mixture in a platinum crucible, and the quenched slag was analyzed by EPMA and wet chemical analysis. The results show low solubility of CaO and SiO<sub>2</sub> in wustite and magnetite phases. This low solubility allows consideration of the precipitated iron oxides as pure phases. Consequently, a relationship between the activity coefficient of iron in the slag system and the content of iron in the platinum crucible was obtained. The results can be expressed by the following equation:

$$\log \gamma_{Fe} = -3.45 + 6.89NFe - 2.29(NFe \text{ (in Pt)})^2 \\ 0.08 < NFe \text{ (in Pt)} < 0.5$$

This equation was used to calculate the activities and activity coefficients of FeO (l) and FeO<sub>1.33</sub> (s) in the liquid region of the phase diagram FeO-Fe<sub>2</sub>O<sub>3</sub>-CaO-SiO<sub>2</sub>. The activity coefficients of FeO (l) were then

**Table XI. Equilibrium between Platinum Crucible and Liquid FeO-Fe<sub>2</sub>O<sub>3</sub>-CaO-SiO<sub>2</sub> Slag at 1623 K and pO<sub>2</sub> of 10<sup>-6</sup> atm**

Number	Mass Pct Fe in Pt	Slag Composition, Mass Pct				Slag Composition, Mol Fraction				Activity and Activity Coefficient		
		Fe	SiO <sub>2</sub>	CaO	Fe <sup>3+</sup> /Fe <sup>2+</sup>	NSiO <sub>2</sub>	NCaO	NFeO	NFeO <sub>1.5</sub>	aFeO <sub>1.33</sub>	aFeO	γ <sub>FeO</sub>
K-1	10.4	63.79	6.90	8.88	0.93	0.07	0.13	0.42	0.39	0.89	0.47	1.14
K-2	10.3	46.71	19.51	17.05	0.60	0.22	0.21	0.36	0.22	0.86	0.46	1.28
K-3	10.2	60.55	15.95	4.05	0.60	0.19	0.05	0.47	0.28	0.84	0.45	0.94
K-4	10.2	59.13	9.90	11.90	0.91	0.12	0.15	0.38	0.35	0.84	0.45	1.17
K-5	10.2	49.76	23.23	10.09	0.48	0.26	0.12	0.41	0.20	0.83	0.44	1.07
K-6	10.2	62.91	17.18	0.00	0.50	0.20	0.00	0.53	0.27	0.83	0.44	0.83
K-7	10.1	47.84	27.25	6.94	0.44	0.31	0.08	0.42	0.18	0.81	0.44	1.02
K-8	10.1	43.77	18.50	21.75	0.90	0.21	0.26	0.28	0.25	0.81	0.43	1.53
K-9	10.1	63.47	3.24	11.08	1.14	0.04	0.14	0.38	0.43	0.80	0.43	1.11
K-10	10.1	61.84	2.75	13.98	1.19	0.03	0.18	0.36	0.43	0.79	0.42	1.18
K-11	10.0	41.49	23.14	22.23	0.70	0.26	0.26	0.28	0.20	0.77	0.41	1.45
K-12	10.0	47.93	31.44	4.38	0.33	0.36	0.05	0.45	0.15	0.76	0.41	0.91
K-13	9.6	25.16	32.83	32.72	0.80	0.34	0.37	0.16	0.13	0.67	0.35	2.21
K-14	8.2	57.87	0.00	21.17	1.73	0.00	0.27	0.27	0.46	0.37	0.20	0.74
K-15	7.7	20.62	45.78	25.54	0.32	0.47	0.28	0.18	0.06	0.31	0.17	0.91

**Table XII. Equilibrium between Platinum Crucible and Liquid FeO-Fe<sub>2</sub>O<sub>3</sub>-CaO-SiO<sub>2</sub> Slag at 1673 K and pO<sub>2</sub> of 10<sup>-8</sup> atm**

Number	Mass Pct Fe in Crucible	Slag Composition, Mass Pct				Slag Composition, Mol Fraction				Activity and Activity Coefficient	
		Fe	SiO <sub>2</sub>	CaO	Fe <sup>3+</sup> /Fe <sup>2+</sup>	NSiO <sub>2</sub>	NCaO	NFeO	NFeO <sub>1.5</sub>	aFeO	γ <sub>FeO</sub>
L-1	20.5	53.5	15.79	11.44	0.35	0.18	0.14	0.50	0.18	0.71	1.41
L-2	20.5	58.12	12.32	10.82	0.42	0.14	0.13	0.51	0.21	0.70	1.37
L-3	20.1	50.38	20.09	14.24	0.37	0.23	0.17	0.44	0.16	0.65	1.48
L-4	19.8	49.73	29.42	5.19	0.20	0.33	0.06	0.50	0.10	0.61	1.21
L-5	19.8	47.57	24.41	11.95	0.28	0.27	0.14	0.46	0.13	0.61	1.33
L-6	19.7	38.63	34.02	15.65	0.26	0.37	0.18	0.35	0.09	0.59	1.67
L-7	19.3	40.12	18.485	24.34	—	—	—	—	—	0.55	—
L-8	19.3	56.37	1.06	21.27	0.57	0.01	0.26	0.46	0.26	0.55	1.20
L-9	19.0	32.92	35.50	20.52	0.27	0.38	0.24	0.30	0.08	0.51	1.70
L-10	18.6	32.89	34.60	23.53	0.30	0.37	0.27	0.28	0.08	0.47	1.68
L-11	18.3	35.89	34.94	16.37	0.36	0.38	0.19	0.32	0.11	0.44	1.34
L-12	17.4	30.81	44.83	13.61	0.18	0.48	0.16	0.31	0.06	0.39	1.28
L-13	17.8	46.94	3.41	32.16	0.97	0.04	0.39	0.29	0.28	0.39	1.34
L-14	17.4	46.12	34.64	3.76	0.22	0.39	0.05	0.46	0.10	0.36	0.78
L-15	17.0	39.25	42.65	5.76	0.15	0.47	0.07	0.40	0.06	0.33	0.82
L-16	16.9	25.56	34.25	29.57	0.68	0.36	0.33	0.18	0.12	0.32	1.76
L-17	16.4	18.32	37.09	36.47	0.46	0.38	0.40	0.15	0.07	0.28	1.87
L-18	16.3	18.28	36.97	37.81	0.44	0.38	0.41	0.15	0.06	0.28	1.92
L-19	13.5	18.82	47.85	25.98	0.41	0.49	0.29	0.15	0.06	0.13	0.84
L-20	9.9	14.32	52.43	26.55	0.30	0.53	0.29	0.13	0.04	0.04	0.30

**Table XIII. Selected Equilibrium Constants**

Reaction	Temperature (°C)	K	Reference	Reference State
Fe (s) + 1/2O <sub>2</sub> (g) = FeO (l)	1573	237,302	17	pure Fe-O melt in equilibrium with γ-Fe
	1623	74,438		
Fe (s) + 2/3O <sub>2</sub> (g) = FeO <sub>1.33</sub> (s)	1573	7,243,045	16	solid crystalline stoichiometric Fe <sub>3</sub> O <sub>4</sub>
	1623	3,037,972		
	1673	1,401,764		

**Table XIV. Equilibrium among Platinum Crucible, Liquid Slag, and Silica at 1573 K and  $pO_2$  of  $10^{-7}$  atm and Platinum Crucible, Liquid Slag, and Dicalcium Ferrite at 1573 K and  $pO_2$  of  $10^{-7}$  and  $10^{-8}$  atm**

Number	Equilibrium	Crucible	Mass Pct				
			Slag			$a_{FeO}$	
			Fe	SiO <sub>2</sub>	CaO		
M-1	platinum crucible, liquid slag, and silica $10^{-7}$ atm	Fe	9.3	50.53	32.2	0	0.31
M-2			9.0	51.10	32.8	0	0.29
M-3	platinum crucible, liquid slag, and $2CaO \cdot Fe_2O_3$ $10^{-8}$ atm	Fe	12.8	52.21	0.01	29.8	0.34
M-4			12.7	52.18	0.06	29.7	0.32
M-5			12.3	50.86	0.83	28.1	0.28
M-6			12.7	53.20	1.15	28.80	0.32
M-7	platinum crucible, liquid slag, and $2CaO \cdot Fe_2O_3$ $10^{-6}$ atm	Fe	5.75	71.49	0	25.5	0.20
M-8			6.1	70.32	0.16	24.2	0.24
M-9			6.2	71.50	0.77	24.8	0.25
M-10			6.1	68.56	2.59	25.6	0.24
M-11			6.1	69.19	2.67	25.2	0.24

determined by the obtained molar fraction compositions of the liquid  $FeO-Fe_2O_3-CaO-SiO_2$  system and the content of iron in the platinum crucible.

The thermodynamic properties derived from the present experimental data reproduce well the thermodynamic information reported in the literature.

The results indicated that the activity coefficient of  $FeO$  ( $\lambda$ ) increases with increasing content of  $CaO$  in the slag. At a given oxygen partial pressure, there is no appreciable change in the isoactivity coefficient lines of  $FeO$  ( $\lambda$ ) when the temperature increases from 1573 to 1673 K. However, at a given temperature, a decrease in the oxygen partial pressure displaces the isoactivity lines toward the  $CaO$  corner.

## REFERENCES

1. M. Timucin and A. Morris: *Metall. Trans.*, 1970, vol. 1, pp. 3193–3201.
2. T. Ogura, R. Fujiwara, R. Mochizuki, Y. Kawamoto, T. Oishi, and M. Iwase: *Metall. Trans. B*, 1992, vol. 22B, pp. 459–66.
3. H. Henao, F. Kongoli, and K. Itagaki: *Mater. Trans.*, 2005, vol. 46, pp. 812–19.
4. B. Zhao, E. Jak, and P.C. Hayes: *Metall. Mater. Trans. B*, 1999, vol. 30B, pp. 597–605.
5. E. Turkdogan: *Trans. AIME*, 1961, vol. 221, pp. 1090–95.
6. E. Turkdogan: *Trans. AIME*, 1962, vol. 224, pp. 294–98.
7. Y. Takeda, S. Nakazawa, and A. Yazawa: *Can. Metall. Q.*, 1980, vol. 19, pp. 297–305.
8. O. Knacke, O. Kubaschewski, and K. Hesselmann: *Thermochemical Properties of Inorganic Substances*, 2nd ed., Springer-Verlag, New York, NY, 1991, p. 309.
9. L. Darken and R. Gurry: *J. Am. Chem. Soc.*, 1945, vol. 67, pp. 1398–1412.
10. L. Darken and R. Gurry: *J. Am. Chem. Soc.*, 1946, vol. 68, pp. 798–816.
11. P. Spencer and O. Kubaschewski: *CALPHAD*, 1978, vol. 21, pp. 47–167.
12. A. Muan: *Trans. AIME, J. Met.*, 1955, Sept., pp. 965–76.
13. W.C. Allen and R.B. Snow: *J. Am. Ceram. Soc.*, 1955, vol. 38, pp. 264–81.
14. R. Taylor and A. Muan: *Trans. AIME*, 1962, vol. 224, pp. 500–02.
15. P. Fredriksson and S. Seetharaman: *Scand. J. Metall.*, 2001, vol. 30, pp. 258–64.
16. *NIST-JANAF Thermochemical Tables*, 4th ed., M.W. Chase, Jr., ed., American Institute of Physics and The American Chemical Society, USA, 1998, p. 1248.
17. R. Schuhmann, Jr. and P.J. Ensio: *Trans. AIME, J. Met.*, 1951, vol. 191, pp. 401–16.
18. *Slag Atlas*, Verein Deutscher Eisenhütten (VDEh), Germany, 1995, pp. 126 and 127.